ELSEVIER

Thin Solid Films 420–421 (2002) 318–323

thin solid films

www.elsevier.com/locate/tsf

Investigation of the residual stresses and mechanical properties of (Cr,Al)N arc PVD coatings used for semi-solid metal (SSM) forming dies

E. Lugscheider, K. Bobzin, Th. Hornig, M. Maes*

Materials Science Institute, Aachen University of Technology, Augustinerbach 4-22, 52056 Aachen, Germany

Abstract

In many cases, high compressive stresses are an unwanted side effect of deposited PVD coatings, because they are known to reduce the adhesive strength of the coating on the substrate. However, in some applications a main focus of the PVD coatings consists of bringing the surface of a substrate into a compressive state. A surface being in a compressive state is more likely to withstand thermal and mechanical alternating stresses within the surface and has a higher resistance against forming cracks and increases the life span of semi-solid metal forming (SSM) dies. Arc ion plating is a PVD process, which is known to cause high compressive stresses in coatings due to its high ionisation rate and the applied bias voltage to the substrate. Therefore, the arc ion plating process is suitable for bringing a surface of a substrate into a compressive state. The investigated (Cr,Al)N coatings were deposited in such an arc ion plating PVD process and the thickness varies from 2.7 to 17 μm. The correlation of thickness vs. residual stresses of these coatings was investigated. In order to determine these residual stresses a stripe bending test is backed up and compared with a XRD stress analysis. Additionally, the coatings were exposed to impact tests to determine the influence of compressive stresses on the wear behaviour caused by alternating stresses.

Keywords: Residual stress analysis; Semi-solid metal forming; Chromium based coating

1. Introduction

The ternary coating (Cr,Al)N combines, compared to other hard materials, a good chemical resistance with a high hardness and melting point. The combination of these properties makes (Cr,Al)N coatings suitable for application on dies for semi-solid metal forming (SSM). SSM is a fairly new metal forming process, which combines the advantages of forging and die casting in a single process. The process is based on the specific rheological behaviour first discovered at the MIT in the early 1970s by Flemming and Spencer [1,2]. Related areas like pressure die casting of aluminium have already shown promising results concerning lifespan increases due to use of hardcoatings on dies [3,4]. An additional high residual compressive stress within the coating or surface in a die is known to enhance the resistance against crack initiation and propagation caused by alternating mechanically- or thermally-induced stresses. Increasing the compressive stress within a coating is therefore a focus of this paper [5].

*Corresponding author. Tel.: +49-241-809-5577; fax: +49-241-809-2264.

E-mail address: maes@msiww.rwth-aachen.de (M. Maes).

2. Experimental

2.1. Deposition process

The investigated coatings were deposited in a Multi Arc PVD 20 system, equipped with two random arc sources, containing a pure chromium and a pure aluminium target each. A single batch contained a H11 (1.2343) hot working steel, a cemented carbide and an annealed stress free bending stripe (1.4310) sample. The last mechanical preparation step consists of polishing the substrates with a 6 μm diamond suspension followed by an ultrasonic cleaning.

The film thickness was varied by the length of deposition time, which resulted in coatings varying from 2.7 to 17 μm with an average deposition rate of 1.1–1.4 nm/s. All other deposition parameters were then kept constant at all batches.

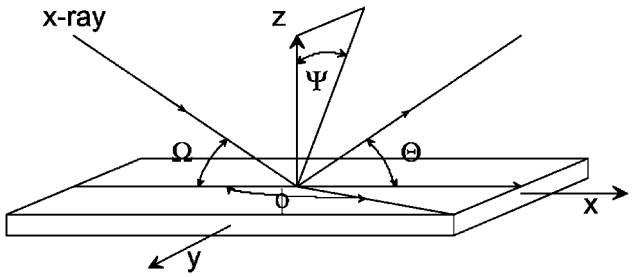

Fig. 1. Co-ordinate system used in X-ray stress analysis.

2.2. Determination of mechanical properties

The mechanical coating properties were analysed using tests such as scratch test, microhardness, nanoindentation and surface roughness [6]. Additionally, impact tests were used to simulate alternating stresses within the surface. The impact tester is a device which offers the possibility to evaluate the resistance of (coated) surfaces [7] against impulsive strain by means of impacting a cemented carbide ball onto a coated surface with a predefined load. The coatings' morphology and impact craters were investigated by means of scanning electron microscopy (SEM).

2.3. Determination of intrinsic stresses by means of bending stripe method

Due to the importance of compressive stresses within the coating, three different ways of determining residual stresses are compared in this paper. First, by using the Stoney [8], secondly by Senderhoff's equation [9] and thirdly, by means of X-ray diffraction techniques.

In order to minimise failure using the bending stripe method, the bent beam has to be clamped in a specific way. The construction of the substrate holder allowed the substrate to expand in the lateral direction, which restricts the substrate to be bent during deposition.

Special demands concerning material properties of the bent beam are met using a spring steel stripe (X12CrNi17-7 or AISI 302) with the dimensions 70 mm×7 mm×0.2 mm, that has little or no plastic deformation in the required temperature range. A bent beam was then mounted on the substrate holder and single sided coated. After cooling the coated bending stripe to room temperature, it should show a perfect bending radius caused by the residual stress.

2.4. Determination phases and intrinsic stresses by means of X-ray diffraction

The in-plane surface residual stress in the coatings were also determined by X-ray diffraction using the $\sin^2 R$ method (Fig. 1).

Prior to the stress analysis, phases were determined by X-ray diffraction. After determining the angle areas (theta and omega) in which a peak occurs, these same areas were then scanned at tilted angles (ϕ and ψ). After removing the background counts and smoothing the reading, the shift of the peaks' centre of gravity position is then calculated by a Pseudo-Voigt fit. It should be mentioned that XRD stress measurements with rather low energetic Co radiation are limited to the near-surface-regions of the coating due to the low X-ray penetration in chromium based PVD coatings, which could cause a problem at higher film thicknesses.

3. Theoretical basis

A common way to adjust the amount of compressive residual stress can be achieved by varying the bias voltage at the substrate, since the arc ion plating process provides a high ionisation rate. The upper limit of the bias voltage is given by spalling of a coating near the edges of the substrate, due to the inhomogenous distribution of the residual stress. A second method of varying the amount of stress can be achieved by changing the total pressure within the vacuum chamber, which significantly changes the mean free path of an atom. A reduction of the mean free path thereby increases the chance of a collision with a second atom and thus changes the average kinetic energy of the ionised particles, which is a main cause of lattice elongation and growth-induced stresses within the coating. A lower limit of the pressure is given by an insufficient nitridation (in case a reactant is nitrogen) of the coating. A third method of adjusting residual stresses within a coating can be done by varying the film thickness, which is the main focus of this paper.

$$\sigma_{\text{residual}} = \sigma_{\text{growth}} + \sigma_{\text{thermomechanical}} + \sigma_{\text{mechanical}}$$

Residual stress within a coating can be divided into three separate classes:

- thermomechanically-induced stresses, these stresses are present when
  - the application temperature differs from the deposition temperature and
  - CTE (coefficients of thermal expansion) values between coating and substrate do not match
- mechanically-induced stresses exist when the substrate is prestressed during deposition
- growth-induced stresses are caused during deposition, when the lattice spacing of the coating is distorted by the high kinetic energy during ion implantation

4. Results

4.1. Film thickness

All coatings show linear growth in film thickness. The only exception is batch 5, which had a layer

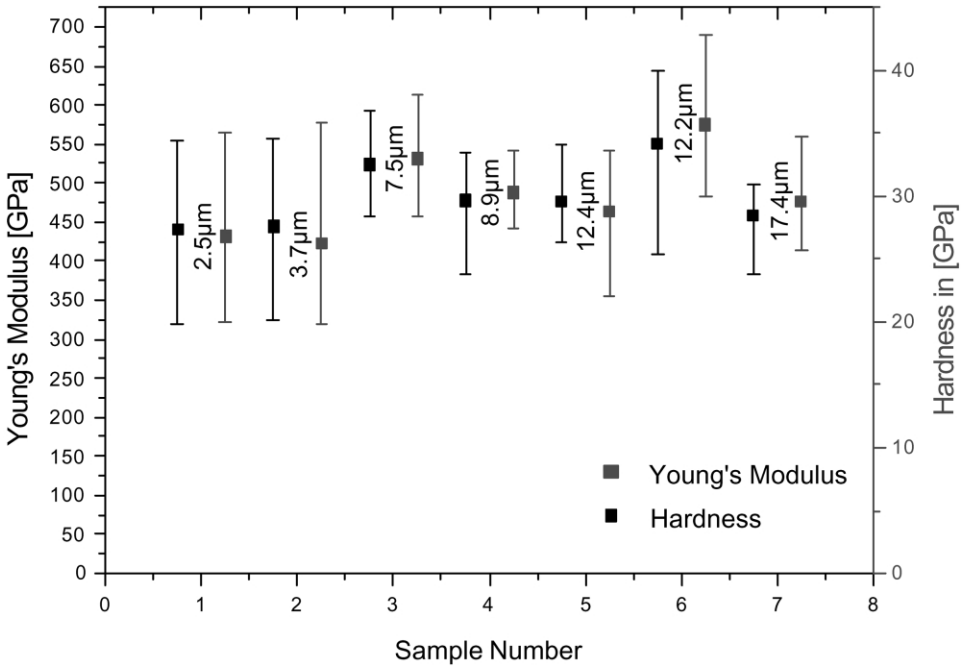

Fig. 2. Nanoindentation, showing Young's moduli and nano hardness.

thickness of 12.2 μm. When comparing batch 5 and 6, the layer thicknesses of both batches are almost equal, although the deposition time of batch 6 was 30 min longer then batch 5. The different fibre texture of this coating due to small differences in deposition parameters, could be responsible for this behaviour. Although a different fibre texture was found in XRD analysis, no conclusions about the lattice (bcc, fcc or hcp), which could influence the deposition rate can be made with the acquired data.

4.2. Scratch test

Highest loads were obtained for cemented carbide samples with a film thickness of 8.9 μm, which showed no signs of any adhesive or cohesive failure. A further increase of the film thickness proved to be useless on a cemented carbide, since maximum scratch loads were lower at higher film thicknesses and showed cohesive failure within the coating, mainly caused by impurities within the coatings' surface.

Caused by the weaker substrate, an increase in film thickness on a H11 or 1.2343 hot working steel proved to have a positive effect in terms of resistance against higher scratch loads. In the latter case the coating's thickness provides a self-supporting layer, which restricts the coating to give way against the high pressure caused by the scratch diamond. In case of the cemented carbide substrate, this self-supporting behaviour is not required because the substrate already has a higher basic hardness (cemented carbide 1600 HV) compared to the much softer hot working steel (HV 600 near surface).

4.3. Hardness

The indentation hardness was measured by nanoindentation. The nanoindents were taken in plane and at constant depth of 300 nm. Results of these nanoindentations are shown in Fig. 2, which shows that Young's modulus and hardness of most samples stay within a certain range. The only exception is sample 6, which shows a different behaviour concerning the Young's modulus and hardness. The cause of this behaviour was again linked to a different fibre texture measured with XRD phase analyses.

4.4. X-Ray analysis

A phase analysis was carried out prior to the X-ray stress analysis. The investigated coatings showed a strong fibre texture, and most of the coatings showed a (111) texture, see Fig. 3. Batch 6 showed in many ways a different behaviour, concerning film thickness, residual stress and spalling during impact tests. Phase analysis proved that this sample had a strong (220) texture. By investigating the coatings' protocols a distinct difference in arc current could be found at the chromium target. This property would have a profound impact on the chromium ion flux, and would lead to the fewer chromium atoms being incorporated in the coating. EDS-Analysis showed that except for batch 6, all batches had an Al-content in the range of 25% and a Cr content of 63% and 11% nitrogen. Batch 6 had an Al-content of 16.24% and a Cr content of 78.93% and 4.82% nitrogen.

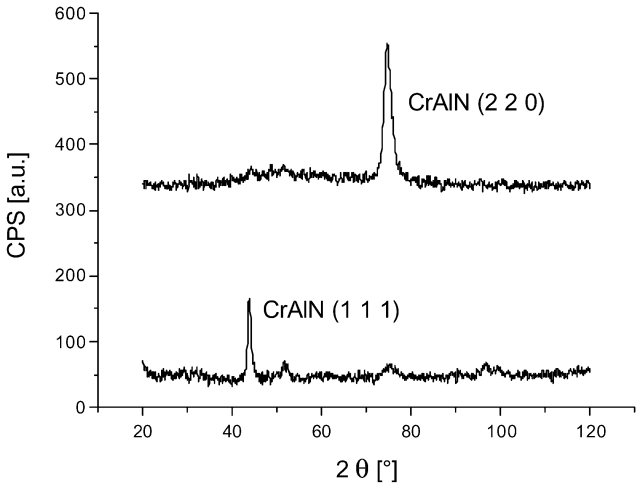

Fig. 3. Phase analysis and fibre texture of batch 5 and 6.

The low amounts of nitrogen are due to the resolution limits of the EDS detector for low atomic numbers.

4.5. Residual stress

A common and easy to use method for determining the residual stress of PVD coatings is given by the Stoney equation. The major advantage of this method is that in order to calculate the amount of residual stress within a coating, the Young's Modulus of the film is not required, provided that the PVD coating is in comparison to its thickness relatively small, e.g. $h_{\text{coating}} \ll h_{\text{substrate}}$ ratio of 1:100.

$$\sigma_{\text{residual stress coating}} = \frac{E_{\text{substrate}} h_{\text{substrate}}^2}{6(1-\nu_{\text{substrate}}) h_{\text{coating}}} \left(\frac{1}{r_b} - \frac{1}{r_a} \right) \quad (1)$$

To ensure that no thermomechanical or mechanical stresses are present within the bending stripe before deposition, the bending stripes were stress-free annealed.

A more accurate stress analysis can be determined by the bending stripe method using Senderhoff's equation, which additionally makes use of the coating's Young's modulus.

$$\sigma_{\text{residual stress coating}} = \frac{E_{\text{substrate}} \left(h_{\text{substrate}} + \frac{E_{\text{coating}}(1-\nu_{\text{substrate}})}{E_{\text{substrate}}(1-\nu_{\text{coating}})} h_{\text{coating}} \right)^3}{6(1-\nu_{\text{substrate}}) h_{\text{coating}} h_{\text{substrate}}} \times \left(\frac{1}{r_b} - \frac{1}{r_a} \right) \quad (2)$$

The Young's moduli needed for this equation were separately determined by nanoindentation for each single batch. This ensures that differences between batches concerning deposition parameters are compensated.

In order to back up this acquired data from the bending stripe method, an X-ray stress analysis was carried out for some of the samples. As mentioned earlier this theory of stress analysis is based on a shift in peak position, when a sample is tilted. For initial measurements, reflexes did not occur in the expected angle ranges. To determine any inconsistencies within the coating's texture a pole figure was then created. The graph of this pole (Fig. 4) shows that the pole of the

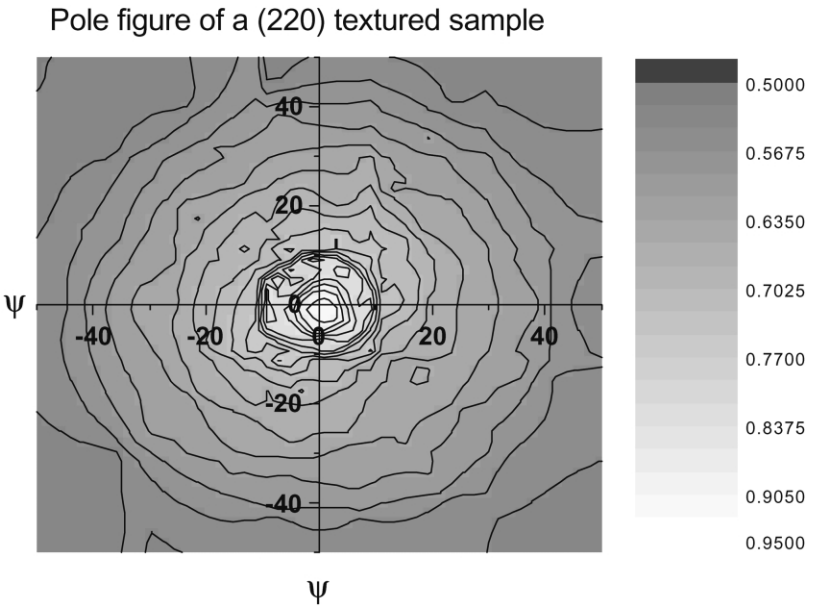

Fig. 4. Pole figure of textured sample from batch 5.

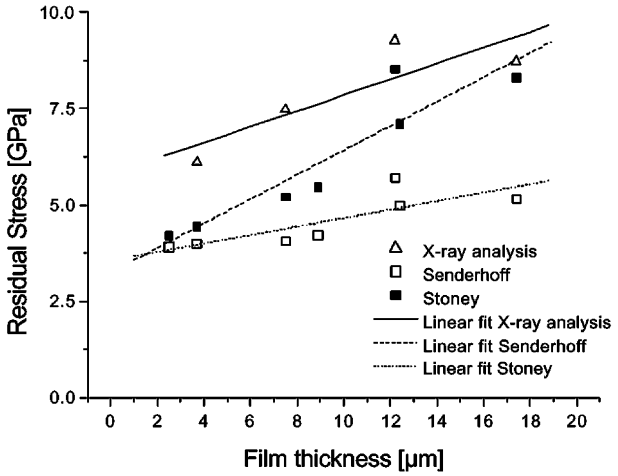

Fig. 5. Residual stress of the investigated coatings.

coating's intensity was shifted and thereby asymmetrical.

Along with this acquired data, a shift of the sample could be determined and taken into account when using an X-ray stress analysis. A possible cause of this shift might be a result of the spatial orientation of the targets within the vacuum chamber, since all samples were coated with a static arrangement.

In order to compensate this asymmetrical property the sample has to be pre-tilted and rotated along the ϕ and ψ axis.

Intrinsic stresses could then be calculated using the following equation:

$$\sigma_{11}-\sigma_{33}=\frac{1}{D_0}\frac{E}{(1+\nu)}\frac{\partial D}{\partial \sin^2\psi} \quad (3)$$

where σ_{11} is a tension component in lateral direction and σ_{33} in the in-plane direction, E is given by the Young's modulus, ν the Poisson's ratio and D_0 the lattice spacing of a stress free sample.

The results of the determination of the residual stress are shown in the Fig. 5. The validity of Stoney equation, with respect to film and substrate thickness ratio (1:100) was not met when the coatings' thickness exceeds 2 µm. Therefore, the error is still small when calculated in the thin film range, but tends to get larger with increasing film thickness. As far as the validity of Senderhoff's equation is concerned, a certain length-to-width ratio has to be met [9].

4.6. Impact tests

All impact tests were carried out on a hot working steel substrate. Although increased film thickness leads to a higher scratch resistance. These coatings showed that increasing film thickness does not lead to improved results when exposed to a high impulsive strain. The samples with a thickness larger than 9 µm and an alternating force of 700 N, all lead to massive spalling within the impact crater (Fig. 6). The cause of this behaviour can be linked to a lack of plasticity within the coating. A thinner coating is better able to follow the impact of a ball and will therefore less likely lead to spalling.

5. Conclusions

Results show that the amount of compressive residual stress increases with increasing film thickness, provided that all deposition parameters, except deposition time are kept constant. Compressive residual stress must be developed by Ion Peening [10,11]. When the deposition process is started, the growing film is still able to relax, since the substrate does not inhibit plastic deformation of the coating. With increasing layer thickness, the

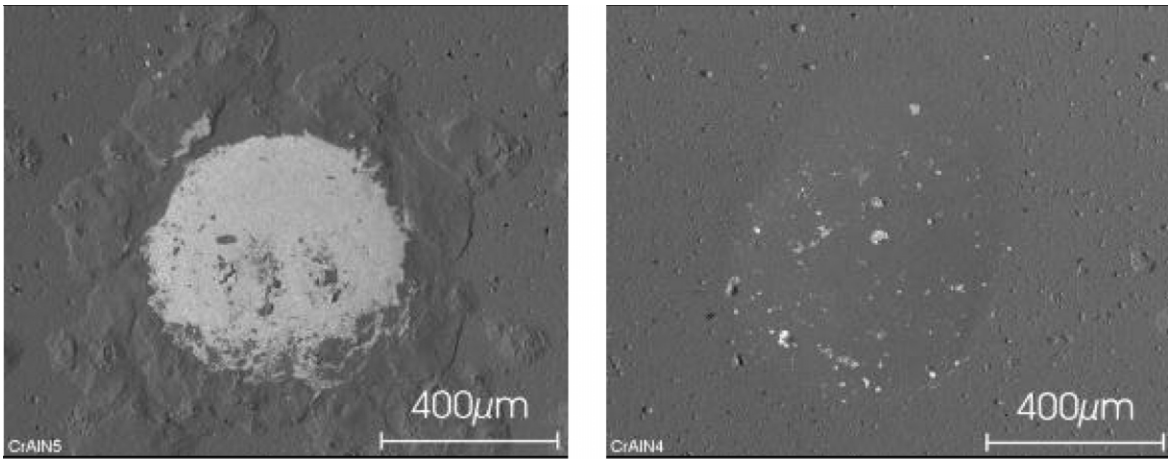

Fig. 6. Impact crater after 100 000 impacts at 700 N, left (12.2 µm), and right (8.9 µm).

DOCKET ALARM

Explore Litigation Insights

Docket Alarm provides insights to develop a more informed litigation strategy and the peace of mind of knowing you're on top of things.

Real-Time Litigation Alerts

Keep your litigation team up-to-date with **real-time alerts** and advanced team management tools built for the enterprise, all while greatly reducing PACER spend.

Our comprehensive service means we can handle Federal, State, and Administrative courts across the country.

Advanced Docket Research

With over 230 million records, Docket Alarm's cloud-native docket research platform finds what other services can't. Coverage includes Federal, State, plus PTAB, TTAB, ITC and NLRB decisions, all in one place.

Identify arguments that have been successful in the past with full text, pinpoint searching. Link to case law cited within any court document via Fastcase.

Analytics At Your Fingertips

Learn what happened the last time a particular judge, opposing counsel or company faced cases similar to yours.

Advanced out-of-the-box PTAB and TTAB analytics are always at your fingertips.

API

Docket Alarm offers a powerful API (application programming interface) to developers that want to integrate case filings into their apps.

LAW FIRMS
Build custom dashboards for your attorneys and clients with live data direct from the court.

Automate many repetitive legal tasks like conflict checks, document management, and marketing.

FINANCIAL INSTITUTIONS
Litigation and bankruptcy checks for companies and debtors.

E-DISCOVERY AND LEGAL VENDORS
Sync your system to PACER to automate legal marketing.